

Impact of Gold Nanoparticle Concentration on their Cellular Uptake by MC3T3-E1 Mouse Osteoblastic Cells as Analyzed by Transmission Electron Microscopy

Thikra Mustafa¹, Fumiya Watanabe¹, William Monroe², Meena Mahmood¹, Yang Xu¹, Lamya Mohammed Saeed¹, Alokita Karmakar¹, Dan Casciano¹, Syed Ali³ and Alexandru S. Biris^{1*}

¹Nanotechnology Center, University of Arkansas at Little Rock, 2801 S. University Ave, Little Rock, AR 72204, United States

²Electron Microscope Center, Mississippi State University, Mississippi State, MS 39762, USA

³National Center for Toxicological Research, Food and Drug Administration, 3900 NCTR Road, Jefferson, AR 72079, United States

Abstract

The uptake mechanisms and kinetics of gold nanoparticles (AuNPs) by mouse calvaria osteoblastic cells have been studied by transmission electron microscopy (TEM). The average size of the as-synthesized AuNPs used in this study was 12.2 (\pm 1.3) nm, and they were used to expose MC3T3-E1 osteoblastic cells at two concentrations (10 and 160 μ g/ml) for 6, 24, and 96 hours before TEM imaging. Based on this analysis, we propose that the uptake mechanism of AuNPs is concentration-dependent. At the higher concentration (160 μ g/ml), the particles seem to penetrate inside the cells primarily by endocytosis as the cells engulf AuNPs as agglomerates formed on the outer cellular membrane. At the lower concentrations of 10 μ g/ml, AuNPs are more likely to cross the plasma membrane individually through diffusion. Therefore, the average diameters of the nanoparticles are expected to have a significant role only when exposed to cells in low concentrations. Moreover, cytotoxicity assays showed no toxic effects of the AuNPs when MC3T3-E1 cells were exposed to concentrations used in the experiments.

Keywords: Gold nanoparticles; Uptake mechanism; MC3T3-E1 mouse osteoblastic cells; Transmission electron microscopy

Introduction

Nanomaterials have great potential for use in biology and medicine given their unique properties, which enable them to be used as active agents in a number of applications ranging from drug [1-3] or gene-delivery [4-6] to tissue engineering. Investigations of the physical and chemical characteristics of nanomaterials that affect their uptake by eukaryotic cells can yield valuable information required for biomedical applications. The shape [7], size [7,8], concentration, surface chemistry [9-12], and electrical charge [13-15] of nanomaterials are some of the relevant parameters to be considered before introducing them into biological systems [16]. The optimization of such experimental parameters is critical because they control the concentration of nanomaterials that will accumulate inside the cell and the corresponding potential for undesired cytotoxic effects. The use of AuNPs for biological and nanomedical applications [17-19] has experienced a significant increase in the last few years due to their excellent biocompatibility, inertness, stability, lack of cytotoxic effects, ability to be functionalized with various biochemical molecules, and strong spectroscopic capabilities [7,18,20]. In addition, the size of AuNPs can easily be controlled during the synthesis by a simple step in the chemical reaction, namely the ratio of gold salt to reducing agents [21]. *In vivo* studies have indicated that AuNPs have the ability to distribute in different organs and tissues within the body [22]; and they can even penetrate subcellular organelles [2].

In spite of the numerous studies mentioned above, a better understanding of AuNP interactions with cells is still needed. So far, only a limited number of studies have utilized TEM to investigate the interaction of nanoparticles with eukaryotic cells. For instance, a study of nanoparticle physical and chemical parameters and their impact on the intercellular uptake of nanoparticles has been conducted using TEM as an observational method [7]. Chithrani et al. [7] studied the size and shape effect of AuNPs taken up by mammalian cells. At the same time, Jiang and his group showed the differences in the uptake of

10 and 40 nm of modified AuNPs at various incubation temperatures [24]. The impact of the surface chemistry of PEG-modified iron oxide nanoparticles on cellular penetration and intracellular accumulation has been investigated by Gupta and Curtis [23]. In addition, TEM has also been used to investigate the stage and mechanism of the cellular internalization of protein-coated AuNPs by using the HeLa cell line as a model system [25]. Thus, TEM provides an excellent tool for in-depth biological sample analysis at the cellular and organ level.

For the present study, we chose MC3T3-E1 cells, originating from mouse osteoblasts, as an animal cell model. This cell line has proven useful for laboratory experiments and has been used extensively as an *in vitro* model to study the effect of nanomaterials on enhancement of the mineralization and proliferation of bone cells [18,26]. The aim of the present *in vitro* cell culture study was to directly observe the interaction of AuNPs with MC3T3-E1 cells and assess the effects of concentration and exposure time on the uptake of AuNPs by TEM.

Materials and Methods

Preparation of gold nanoparticles

Gold nanoparticles were prepared by the citrate reduction of HAuCl₄ following the method of Turkevich et al. [27]. Prior to synthesis, a round-bottomed flask equipped with condenser was cleaned in aqua

***Corresponding author:** Alexandru S. Biris, Nanotechnology Center, University of Arkansas at Little Rock, 2801 S. University Ave, Little Rock, AR 72204, USA, Tel: (501) 683-7458; Fax: (501) 683-7601; E-mail: asbiris@ualr.edu

Received September 03, 2011; **Accepted** November 04, 2011; **Published** November 08, 2011

Citation: Mustafa T, Watanabe F, Monroe W, Mahmood M, Xu Y, et al. (2011) Impact of Gold Nanoparticle Concentration on their Cellular Uptake by MC3T3-E1 Mouse Osteoblastic Cells as Analyzed by Transmission Electron Microscopy. J Nanomedic Nanotechnol 2:118. doi:10.4172/2157-7439.1000118

Copyright: © 2011 Mustafa T, et al. This is an open-access article distributed under the terms of the Creative Commons Attribution License, which permits unrestricted use, distribution, and reproduction in any medium, provided the original author and source are credited.

regia (3HCl: HNO₃) and later rinsed thoroughly with de-ionized (DI) water. 0.1 g of HAuCl₄·3H₂O (≥99.9% Aldrich) was dissolved in 400 ml DI water. The solution was heated to boiling temperature while vigorously stirring. A freshly prepared 50 ml of 1% trisodium citrate dehydrate was added to the solution, and the solution was kept at boiling temperature for an additional 20 min. It was then left to cool to room temperature; finally, the volume was adjusted to 500 ml by adding DI water. The final colloidal solution was wine red with a gold concentration of ~ 0.5 mM.

Nanoparticle characterization

As synthesized, AuNPs were characterized by TEM, JEM-2100F (JEOL USA, Peabody, Massachusetts) with an accelerating voltage of 80kV. TEM grids were prepared by depositing a few drops of as prepared colloidal AuNP solution onto holey-carbon coated copper grids which were then allowed to dry for 15 minutes on filter paper. X-ray energy dispersive spectroscopy (XEDS) was performed to confirm the composition of the AuNPs. The images then were observed by TEM using Digital Micrograph (Gatan, Inc, Pleasanton, CA) software to measure the size of the nanoparticles. The variation (mean and standard deviation) for the nanoparticles' diameters was obtained after analyzing over 50 nanoparticles in random fields of view. The AuNP radius was also determined by ultraviolet and visible (UV-Vis) spectrophotometer (Shimadzu UV-3600).

Cell culture

The osteoblast mouse cell line (MC3T3-E1) used in this study was obtained from the American Type Culture Collection (ATCC). The cells were seeded in Polycarbonate membrane Nunc CC Insert (EMS, Hatfield, PA) at a density of 25x10³ cells/well. The tissue culture insert was fitted into 24-well plates. 10 or 160µg/ml of AuNPs were freshly mixed with the alpha minimum essential medium supplemented with 10% fetal bovine serum and 1% penicillin streptomycin antibiotic. The cells were incubated for 6, 24, and 96 hr at 37°C in a 5% CO₂ humidified incubator. After the incubation, the medium with AuNPs was removed from each well and replaced with a fixative solution of 3% glutaraldehyde. Cells incubated with AuNPs-free medium were considered as control samples.

MTT based cytotoxicity assay

The CytoSelect™ cell viability and cytotoxicity assay kit was used to evaluate the cytotoxicity of AuNPs on the osteoblast cells. The cells were seeded in 96-well plates at a density of 25x10³ cells/well. The samples' optical absorbance was normalized to the percent of the negative control, and the provided cytotoxic saponine solution was used as a positive control to compare with our data. The cells were incubated with 1, 10, 100, or 200µg/ml of AuNPs for 24 hr for this assay. Before adding MTT reagent, the cells were washed twice with fresh cold culture medium. 100µL of fresh medium were added with 10µL of MTT reagent to each well, and the cells were incubated overnight at 37°C. Once the purple precipitation was clearly visible in each well, 100µL of detergent solution were added to each well. The cells were incubated for 4 hr in the dark after being covered with aluminum foil. The absorbance of each well at 570 nm was measured by using a microtiter plate reader (BioRad, iMark, USA).

Lactic dehydrogenase (LDH)-release based cytotoxicity assay

LDH release was measured using the LDH assay kit (Cayman Chemicals, Ann Arbor, MI, USA) to evaluate cell membrane integrity. The values of the LDH released by the cells and found in the culture

supernatants were determined by a coupled enzymatic assay that results in the conversion of a tetrazolium salt into a brightly colored formazan product that absorbs strongly at 490nm. MC3T3-E1 cells were seeded in a 96-well plate at a density of (25x10³ cells/well) and incubated with increasing amounts of AuNPs (1, 10, 100 and 200 µg/ml) freshly dispersed in culture medium for 24 hr. Next, 120 µL of supernatant were transferred into 1.5 ml tubes and centrifuged for 5 min at a speed of 400 g. 100 µL of the supernatant were transferred to new 96-well plates, followed by the addition of 100 µL of LDH reaction solution. The plates were incubated for 30 min at room temperature on an orbital shaker. A colorimetric absorbance was recorded at 490 nm using a microplate reader for colorimetric detection (BioRad, iMark, USA).

Cell specimen preparation for TEM

Cells were cultured and exposed to gold nanoparticles (AuNPs) at a dilution of (10 and 160 µg/ml) for 6, 24, and 96 hr, respectively. A control sample was also processed. Samples were fixed in 3% glutaraldehyde fixative in 0.1M phosphate buffer, pH 7.2 for overnight at 4 degrees C. After fixation, all of the samples were thoroughly rinsed with a 0.1 M phosphate buffer (pH 7.2), post-fixed in 2% OsO₄ in 0.1 M phosphate buffer for 2 hr, followed by rinsing in distilled water, and dehydrated in an ethanol solution. The resulting dried specimens were embedded in Spurr's resin which was polymerized at 70°C for 15 hr. Semi-thin sections with thickness of 0.5-1.0 µm along with thin sections -thickness 60-100 nm- were generated for light microscopy and transmission electron microscopy analysis. Thin sections mounted on 200 mesh copper grids were stained with uranyl acetate and lead citrate for transmission electron microscopy and examined and photographed in a JEOL 100 CX II TEM (JEOL USA, Peabody, Massachusetts) at 80 kV. These thin TEM specimens were very stable at less than X100,000 magnification under the microscope, which was definitely suitable for imaging biological samples. Without minimum dosage setup, no degradation of the specimens was noticed. Ion beam sputtered carbon thin film coatings (<2nm) on these sections can improve the stability greatly.

Time-dependent clustering of AuNPs

AuNPs with a concentration of 160 µg/ml were incubated with cell-free medium. TEM grids were prepared by dripping a few drops of the above solution starting from a minimum of 1 min to a maximum of 5760 min. The samples were visualized under JEM-2100F (JEOL USA, Peabody, Massachusetts) at 80 kV. More than 200 AuNPs clusters at each incubation period were observed for statistical analysis of clustering, and the mean cluster size and its standard deviation were calculated.

Results

Characterization of gold nanoparticles

As-synthesized AuNPs had a spherical shape, were mono-dispersed, and showed an excellent colloidal stability (Figure 1a). The corresponding XEDS spectrum indicated peak signals of Au (Figure 1b) at 80keV. The mean particle diameter of as-synthesized AuNPs determined by TEM was 12.2 ± 1.3 nm (Figure 1a inset). Moreover, a strong characteristic plasmon absorption peak at 520 nm corresponding to AuNP diameter of ~12nm was present in the UV-Vis spectrum (Figure 1c).

Cytotoxicity assays

The purpose of the assays for this part of the study was to assess the biocompatibility and the undesirable cytotoxic effects of the nanomaterials on MC3T3-E1 cells *in vitro*. A dye-based colorimetric

assay (MTT) was used to evaluate in a rapid and preliminary manner the cellular cytotoxicity and mitochondrial functional changes induced by the nanoparticles. The principle of this assay is based on the ability of the mitochondrial reductase enzymes system, which is succinate-tetrazolium reductase, to convert the yellow dye 3-(4,5-dimethylthiazol-2-yl)-2,5-diphenyl tetrazolium bromide (MTT) to an insoluble purple-colored formazan crystal in living cells. After 24 hr of exposure to (1, 10, 100 and 200 µg/ml) of AuNPs, the sample's absorbance was normalized to the percent of the negative control, and the provided cytotoxic saponin solution was used as a positive control with which to compare our data. Interestingly, we found that the MC3T3 cells' viability remained unchanged over the wide range (0~200 µg/ml) of AuNPs concentration after 24 hr (Figure 2a).

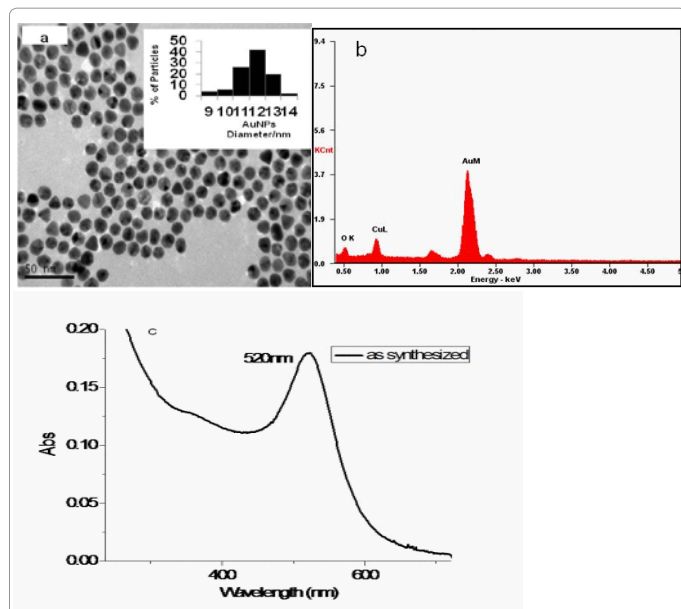


Figure 1: Characterization of AuNPs (a) a TEM image showing monodispersed AuNPs and the size distribution (inset) indicating that the majority of the particles have a size dimension of 12nm, (b) the corresponding XEDS spectrum, and (c) UV-Vis absorbance showing an absorption peak at 520 nm.

Cell viability and plasma membrane integrity were tested by LDH release assay. Lactate dehydrogenase is released into the surrounding medium upon cell damage or lysis. In our study, significant LDH release was noted after a 24 hr incubation period for MC3T3 cells at the highest concentration of AuNPs (200 µg/ml) (Figure 2b). At lower concentrations (<200 µg/ml), gold nanoparticles had no significant effect upon the enzymatic release. To investigate the internalization study, we chose two concentrations of AuNPs with vast differences between them. The lower concentration, 10 µg/ml, showed no cytotoxicity when measured by both assays, while the higher concentration, 160 µg/ml, resulted in a response somewhere between those of the 100 and 200 µg/ml samples.

Uptake mechanisms of AuNPs by the Cells

The main goal of our study was to examine the uptake mechanisms of AuNPs (with an average size of 12.2 ± 1.3 nm) by MC3T3-E1 cells. The effects of the particle concentration and the incubation periods were also examined by incubating the cells with low and high concentrations (10 or 160 µg/ml) of AuNPs for 6, 24, and 96 hr. For cells exposed to the lower concentration of particles, some free aggregates were observed in the cytoplasm of the cells while others were enclosed within membrane vesicles. When these results were compared to the higher concentration, the aggregates appeared smaller and consisted of fewer particles. At 24 and 96 hr incubation periods, more internalized particles were found than at 6 hrs [Compare Figure 3(b) and (c) with 3(a)]. Contrary to the results found at the higher concentration, no AuNPs aggregates were observed attached to the apical surfaces of the plasma membranes.

At the higher concentration of gold particles, at each sampling time (6, 24, and 96 hr), endosomal vesicles of AuNPs could readily be observed, and more than one vesicle containing AuNPs was observed within a single cell as shown in Figure 3(d-f). Internalized vesicles contained only large aggregates of particles, and the aggregated particles appeared mainly inside the vesicle while a few aggregates were free and located in the cytoplasm of the cell. Some of the extracellular AuNP clusters were attached to the surfaces of the cell plasma membrane, while more clusters settled on the apical surface of the plasma membrane of MC3T3-E1 cells as the exposure time increased. Interestingly, the apical surface of the cells was covered with large aggregates of gold nanoparticles after 96 hr of incubation [Figure 3(f) and inset].

The time-dependence of AuNP cluster size in the control experiments without cells was also studied to elucidate the role of the clustering in the biological solution. We chose the concentration of 160 µg/ml for the AuNPs since, generally, the higher the nanoparticles concentration, the higher their tendency to form large aggregates.

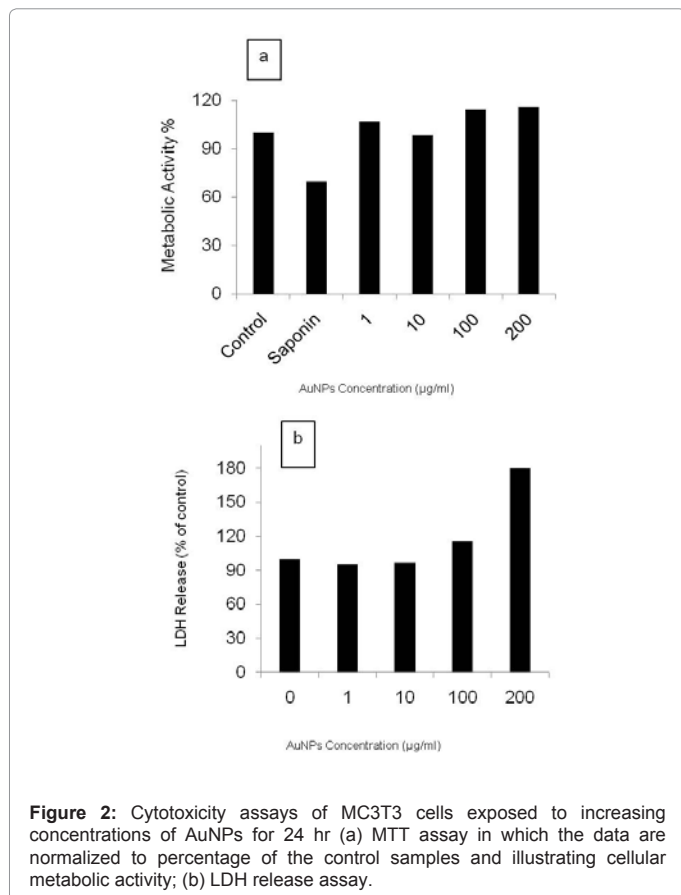


Figure 2: Cytotoxicity assays of MC3T3 cells exposed to increasing concentrations of AuNPs for 24 hr (a) MTT assay in which the data are normalized to percentage of the control samples and illustrating cellular metabolic activity; (b) LDH release assay.

Particles were incubated for a minimum time of 1 min and a maximum of 96 hours in the culture medium free of the cells. Even though the scatter in the data was large, the results showed no significant changes in the average cluster size with increased incubation time [Figure 4]. Therefore, we can conclude that the larger AuNP clusters found on the cell surfaces at the longest incubation time of 96 hr are not due to the particle agglomeration in the medium, but are the results of aggregation to the cell surfaces.

Discussion

Cytotoxicity characterization

MTT and LDH assays were conducted to detect early cytotoxic events. After 24 hr of exposure, no significant cytotoxicity was noticed for any concentration that we used in the uptake study [Figure 2 (a) and (b)]. These results suggest that AuNPs showed no detectable cytotoxicity and essentially did not interrupt cellular function. Patra and colleagues have reported cell type dependent response to AuNPs; they demonstrated that HepG2 and BHK21 cell lines remained unaffected by AuNP treatment, while gold nanoparticles induced cell death in an A549 cell line [28]. In contrast, Pan and coworkers have demonstrated that the cytotoxicity of modified gold nanoparticles is dependent on the size and not on a particular ligand attached to them [29]. Smaller particle size (1-2 nm) was found to be highly toxic, while larger sizes were comparatively nontoxic. Hypothetically, the smaller particles could bind to DNA or other molecular machinery and thereby

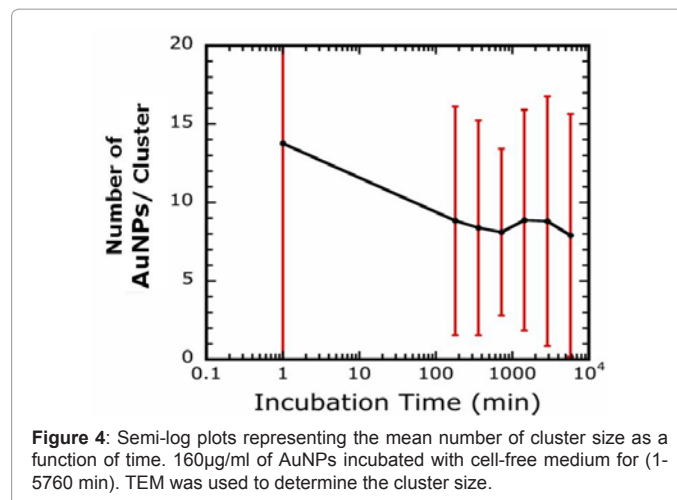


Figure 4: Semi-log plots representing the mean number of cluster size as a function of time. 160µg/ml of AuNPs incubated with cell-free medium for (1-5760 min). TEM was used to determine the cluster size.

block various transcription processes [30]. All of the TEM micrographs in our study indicated that the cells, even those treated with a high concentration of AuNPs, were metabolically active, and the subcellular organelles were morphologically intact prior to fixation for microscopy. The cells had intact plasma membranes and mitochondria, as well as prominent rough and smooth endoplasmic reticulum. Moreover, the ribosomal systems were intact indicating that the cells were active in protein synthesis. As confirmed by the results of cytotoxicity assays and the TEM observations, AuNPs had no significant toxic effect on the MC3T3 cells under the assay conditions we employed in this study.

Uptake of gold nanoparticles

The particles as determined by the TEM were uniform in size, mostly spherical, and free from agglomeration before introduction into the biological medium. MC3T3-E1 grown on cell culture inserts offers a free apical surface of plasma membrane to interact with the extracellular environment while the opposite side is attached to the membrane. For electron microscopy examination, vertically cut sections were collected to show the interaction of the apical side of the cells with AuNPs and the internalization of membrane-coated vesicles within the cell cytoplasm.

Cells exposed to the lower concentration of AuNPs (10 µg/ml) were found to have small clusters of AuNPs localized in the cell cytoplasm indicating the possibility of different uptake mechanisms. The intercellular vesicles are smaller and less numerous at this concentration as compared to those found in the higher concentration (160 µg/ml) cases. After 24 and 96 hr of incubation, more AuNPs were internalized compared to those found after 6 hr incubation at this lower concentration as expected. However, no AuNPs were found to be attached to the apical surface of the plasma membranes even after the longest exposure time [Figure 3(c)]. Since endocytosis usually requires the particles to be adsorbed on the cell surfaces, the AuNPs found inside the cells may have penetrated individually into the cells rather than by endocytosis at this concentration. Geiser et al. [31] have previously detected the ability of nanomaterials to cross the plasma membrane of inhibited phagocytic activity cells and enter the cytoplasm by a non-phagocytic mechanism. Moreover, a similar conclusion was found with cells that lack endocytotic activity (e.g., RBCs) using different types of nanoparticles, gold and titanium oxide of 25 and 22 nm, respectively [31,32].

The cells exposed to the higher concentration of particles (160 µg/ml)

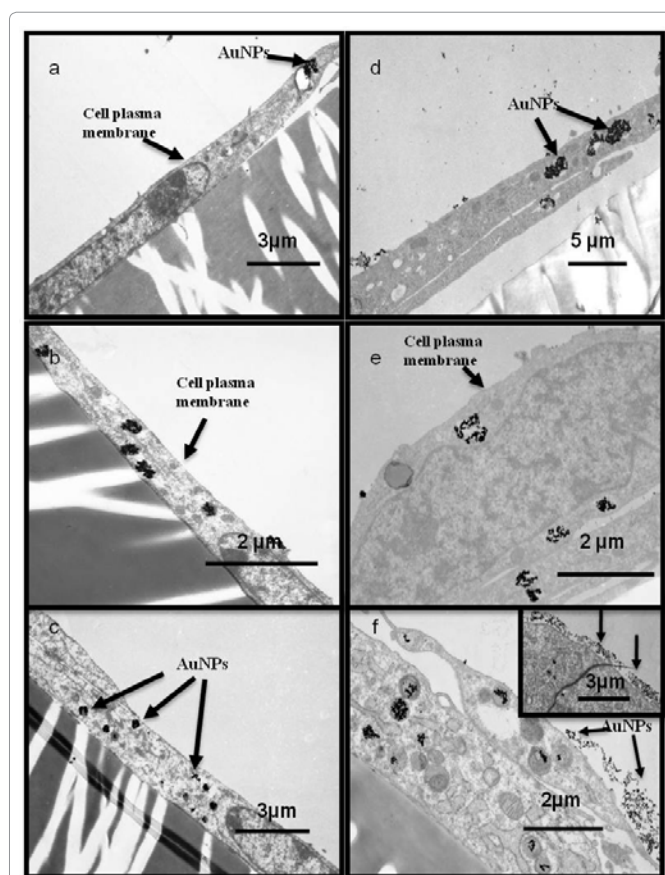
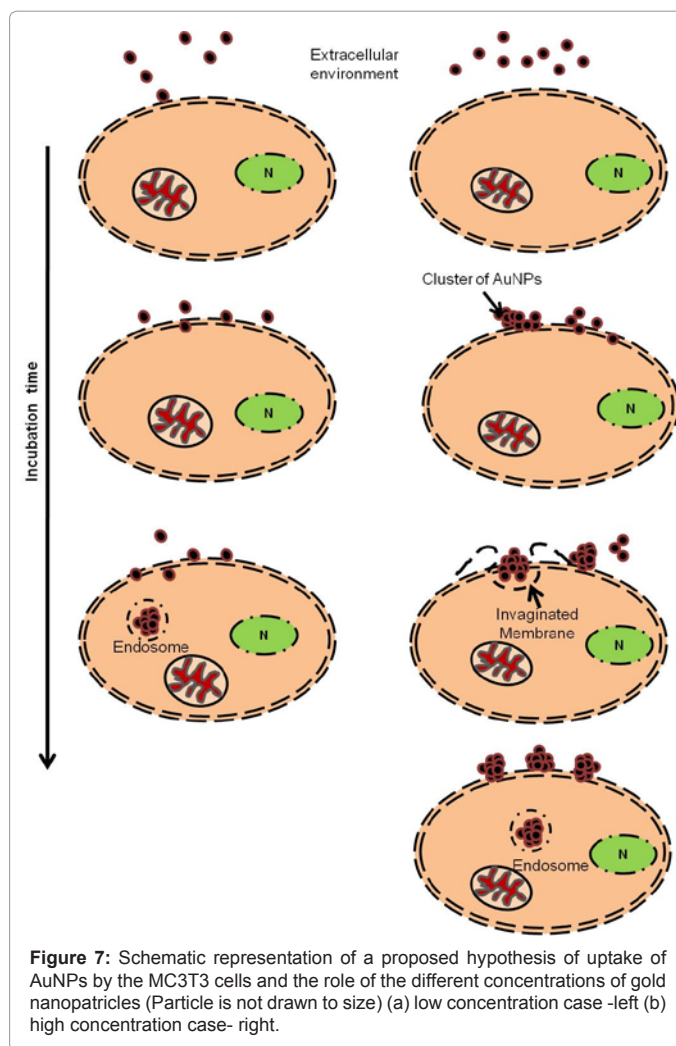
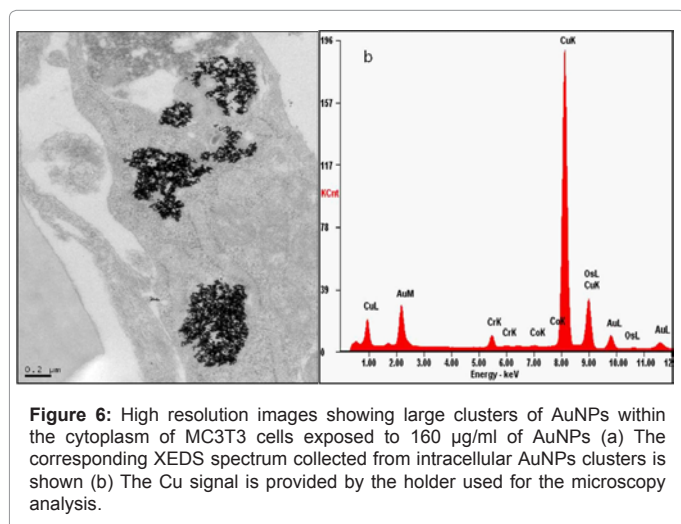
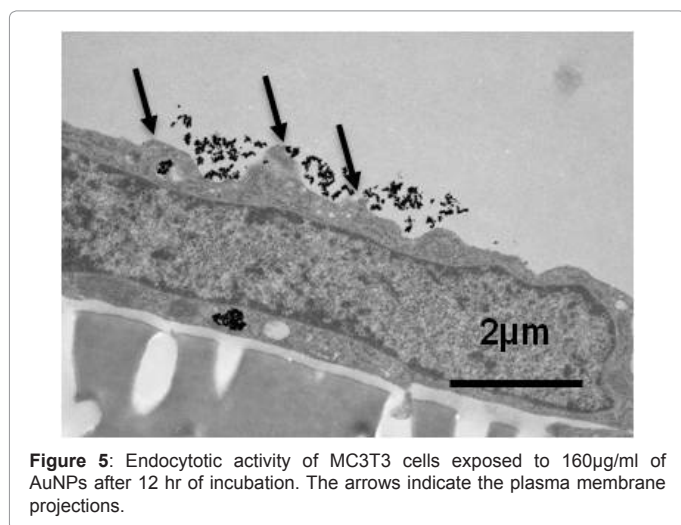


Figure 3: A series of TEM images of MC3T3 cells exposed to 10µg/ml (left column) and 160 µg/ml (right column) of AuNPs after 6 (a and d), 24 (b and e), and 96 (c and f) hr of incubation.

were more likely taken up as clusters; the internalized agglomerates were found within the cytoplasm of the cells, and they were enclosed inside vesicles. Figure 5, which was taken from the cells incubated for 12 hr at 160 µg/ml, clearly shows plasma membrane projections surrounding and engulfing these aggregates of particles before internalization into the cell cytoplasm. The apical surface of the cell plasma membrane appears uneven. Furthermore, different stages of endocytosis are highlighted by the TEM analysis. The images show early endocytosis as the cells surround the AuNPs clusters and the plasma membrane invaginates inward. Additionally, internalized nanoparticle clusters can be observed in the cell cytoplasm, presumably representing later endocytosis. We hypothesize that the ingesting process of large clusters primarily occurred by an endocytotic process, a process by which cells communicate and internalize extracellular contents and solid materials [33]. During the transportation process, foreign materials entered the cells by the invagination of a small portion of the plasma membrane, and then the invaginated part pinched off to form a new intracellular vesicle. Since the cells going through the endocytotic process show a temporary change in the membrane integrity, as the cell membrane expands and finally detaches from the boundary membrane, this could explain the increase in the LDH levels when the concentration of AuNPs reached values higher than 100 µg/ml. A similar mechanism has been suggested in one of the *in vitro* studies with the human epithelial



cell line A549 exposed to 40µg/ml of 50 nm TiO₂ nanoparticles [34]. The aggregation of nanoparticles depends strongly on their surface chemistry [32]. In our experiments, the AuNPs were sonicated before the experiment for maximum dispersion. It seems that the dispersion of the NPs is a function of the environment; it is also possible that the chemical characteristics (e.g., surface properties and charge) of AuNPs change as a result of mixing with the biological solution. This could be due to non-specific absorption of serum proteins on the surface of nanoparticles as demonstrated earlier [35,36]. The surface attachment of these proteins onto the nanoparticles could impact and enhance the endocytotic pathway of the agglomerated AuNPs into the cells. Exposure to high concentrations of AuNPs (160µg/ml) induces their rapid agglomeration on the cell surfaces, and the cells internalize of these large agglomerates. Our TEM study showed the ability of cells to uptake large clusters which formed on the apical surface of cell plasma membranes by endocytosis. The XEDS spectrum collected from intracellular vesicles showed the Au signals [Figure 6 (a) and (b)]. Another possible mechanism for internalization that we propose at the higher concentration is that, since some of the gold clusters were found freely in the cell cytoplasm, single particles may penetrate inside the cell individually by a diffusion process similar to the scenario proposed for the lower concentration study. The predominant mechanism for translocation of AuNPs at such high concentration is more likely through endocytosis.

A previous study by Chithrani et al. showed that the shape [7] of AuNPs (e.g., rod shape vs. spherical shape) played a critical role in intracellular engulfing and accumulation of nanoparticles, while Osaki and colleagues [8] demonstrated that the endocytotic process is highly size-dependent, with an optimal size around 50nm.

Based on our findings, it can be concluded that the size of the nanoparticles plays only a limited role in their uptake by the cells, and it is significant mostly for lower concentrations. As the nanomaterials' concentration increases, they form agglomerates on the cellular membrane and seem to be internalized as a cluster, rather than individually. As a result, the size of the individual nanoparticles that form this cluster becomes rather insignificant. A process diagram is depicted in Figure 7 and highlights the role of the nanoparticles' concentration on their cellular uptake. It is interesting to note that, even after the progression of incubation times and the particles being concentrated in the area surrounding the nucleus, no visible penetration was apparent in the nuclear region. The reason may be related to the structure of the nuclear envelope, which consists of two membrane layers. These findings could play a major role in the design of efficient processes that use nanostructural materials for drug and gene delivery to reduce or eliminate tumors. Therefore, understanding how the engineered nanoparticles interact with various cell lines and in particular with the corresponding cellular membranes is a very important research endeavor, especially given the fact that, in addition to the nanoparticles' size, chemical surface, and shape, their concentration seems to drastically affect the uptake mechanisms by which they penetrate the cells.

Conclusions

Our data suggest that the cellular uptake mechanism of AuNPs is a concentration-dependent process. High concentrations of gold nanoparticles can accumulate more effectively inside and outside of the cells, even in the absence of any functionalization. In addition, viability assays showed no significant cellular toxicity after ingesting AuNPs in the concentration range that we studied. Finally, electron microscopy presents a workable option for investigators studying the interactions between cells and NPs in the environment. TEM observation can distinguish those NPs inside the cells and those on the cell surfaces, as well as the state of agglomeration (NP distribution and cluster sizes) in both cases. A TEM study is in progress to assess the effects of these factors on the ablation of cancerous cells by magnetic NPs.

Acknowledgements

Support for this research received from the Arkansas Science and Technology Authority (ASTA) grant # 08-CAT-03 is greatly appreciated. The financial support provided by the US Army TATRC program is highly appreciated.

References

1. Harjanto D (2006) Gold nanoparticle-assisted delivery of TNF- α in thermal treatments of cancer. *Nanin Reu Research Accomplishments*: 8-9.
2. Kang B, Mackey M, El-Sayed M (2010) Nuclear targeting of gold nanoparticles in cancer cells induces DNA damage, causing cytokinesis arrest and apoptosis. *J Am Chem Soc* 132: 1517-1519.
3. Kirui D, Rey D, Batt C (2010) Gold hybrid nanoparticles for targeted phototherapy and cancer imaging. *Nanotechnology* 21: 1-10.
4. Singh R, Pantarotto D, McCarthy D, Chaloin O, Hoebeke J, et al. (2005) Binding and condensation of plasmid DNA onto functionalized carbon nanotubes: Toward the construction of nanotube-based gene delivery vectors. *J Am Chem Soc* 127: 4388-4396.
5. Ladeira M, Andrade V, Gomes E, Aguiar C, Moraes E, et al. (2010) Highly efficient siRNA delivery system into human and murine cells using single-wall carbon nanotubes. *Nanotechnology* 21: 385101-385112.
6. Karmakar a, Bratton S, Dervishi E, Ghosh a, Mahmood M, et al. (2011) Ethylenediamine functionalized-single walled nanotube (f-SWNT)-assisted *in vitro* delivery of oncogene suppressor p53 gene to breast cancer MCF-7 cells. *Int J Nanomedicine* 6: 1045-1055.
7. Chithrani B, Ghazani A, Chan W (2006) Determining the size and shape dependence of gold nanoparticle uptake into mammalian cells. *Nano Letters* 6: 662-668.
8. Osaki F, Kanamori T, Sando S, Sera T, Aoyama Y (2004) A quantum dot conjugated sugar ball and its cellular uptake on the size effects of endocytosis in the subviral region. *J Am Chem Soc* 126: 6520-6521.
9. Thorek D, Chen A, Czupryna J, Tsourkas A (2006) Superparamagnetic iron oxide nanoparticle probes for molecular imaging. *Ann Biomed Eng* 34: 23-38.
10. Peng XH, Qian X, Mao H, Wang AY, Chen ZG, et al. (2008) Targeted magnetic iron oxide nanoparticles for tumor imaging and therapy. *Int J Nanomedicine* 3: 311-321.
11. Mahmood M, Xu Y, Li Z, Dervishi E., Ali N, et al. (2009) Graphitic materials for RF thermal ablation of tumors. *IEEE* 45: 2162 - 2169.
12. Yang L, Mao H, Wang Y, Cao Z, Peng X, et al. (2009) Single chain epidermal growth factor receptor antibody conjugated nanoparticles for *in vivo* tumor targeting and imaging. *Small* 5: 235-243.
13. Lee KD, Nir S, Papahadjopoulos D (1993) Quantitative analysis of liposome-cell interactions *in vitro*: Rate constants of binding and endocytosis with suspension and adherent J774 cells and human monocytes. *Biochemistry* 32: 889-899.
14. Zhang Y, Yang M, Portney N, Cui D, Budak G, et al. (2008) Zeta potential: A surface electrical characteristic to probe the interaction of nanoparticles with normal and cancer human breast epithelial cells. *Biomedical Microdevices* 10: 321-328.
15. Chenevier P, Veyret B, Roux D, Henry-Toulme N (2000) Interaction of cationic colloids at the surface of J774 cells: A kinetic analysis. *Biophysical Journal* 79: 1298-1309.
16. Zhang Y, Xu Y, Li Z, Chen T, Lantz S, et al. (2011) Mechanistic toxicity evaluation of pristine and PEGylated single-walled carbon nanotubes in neuronal PC12 cells. *ACS Nano* 5: 7020-7033.
17. Mukherjee P, Bhattacharya R, Wang P, Wang L, Basu S, et al. (2005) Antiangiogenic properties of gold nanoparticles. *Clinical Cancer Research* 11: 3530-3534.
18. DanDan L, Jinchao Z, ChangQing Y, Mengsu Y (2010) The effects of gold nanoparticles on the proliferation, differentiation, and mineralization function of MC3T3-E1 cells *in vitro*. *Chinese Science Bulletin* 55: 1013-1019.
19. Zhang Z, Ross RD, Roeder RK (2010) Preparation of functionalized gold nanoparticles as a targeted X-ray contrast agent for damaged bone tissue. *Nanoscale* 2: 582-586.
20. Connor E, Mwamuka J, Gole A, Murphy C, Wyatt M (2005) Gold nanoparticles are taken up by human cells but do not cause acute cytotoxicity. *Small* 1: 325-327.
21. Frens G (1973) Controlled nucleation for the regulation of the particle size in monodisperse gold suspensions. *Nature Physical Science* 241: 20-22.
22. De Jong WH, Hagens WI, Krystek P, Burger MC, Sips AJ, et al. (2008) Particle size-dependent organ distribution of gold nanoparticles after intravenous administration. *Biomaterials* 29: 1912-1919.
23. Gupta AK, Curtis AS (2004) Surface modified superparamagnetic nanoparticles for drug delivery: Interaction studies with human fibroblasts in culture. *J Mater Sci Mater Med* 15: 493-496.
24. Jiang W, Kim BY, Rutka JT, Chan WC (2008) Nanoparticle-mediated cellular response is size-dependent. *Nat Nanotechnology* 3: 145-150.
25. Chithrani BD, Chan WC (2007) Elucidating the mechanism of cellular uptake and removal of protein-coated gold nanoparticles of different sizes and shapes. *Nano Lett* 7: 1542-1550.
26. Mahmood M, Li Z, Casciano D, Khodakovskaya MV, Chen T et al. (2010) Nanostructural materials increase mineralization in bone cells and affect gene expression through miRNA regulation. *J Cell Mol Med* 15: 2297-2306.

27. Turkevich J, Stevenson P, Hillier J (1951) A study of the nucleation and growth processes in the synthesis of colloidal gold. *Discuss Faraday Soc* 11: 55-75.
28. Patra Hk, Banerjee S, Chaudhuri U, Lahiri P, Dasgupta AK (2007) Cell selective response to gold nanoparticles. *Nanomedicine* 3: 111-119.
29. Pan Y, Neuss S, Leifert A, Fischler M, Wen F et al. (2007) Size-dependent cytotoxicity of gold nanoparticles. *Small*: 1941-1949.
30. Liu Y, Meyer-Zaika W, Franzka S, Schmid G, Tsoi M, et al. (2003) Gold-cluster degradation by the transition of B-DNA into A-DNA and the formation of nanowires. *Angewandte Chemie* 42: 2853- 2857.
31. Geiser M, Rothen-Rutishauser B, Kapp N, Schürch S, Kreyling W, et al. (2005) Ultrafine particles cross cellular membranes by nonphagocytic mechanisms in lungs and in cultured cells. *Environ Health Perspect* 113: 1555-1560.
32. Rothen-Rutishauser BM, Schürch S, Haenni B, Kapp N, Gehr P (2006) Interaction of fine particles and nanoparticles with red blood cells visualized with advanced microscopic techniques. *Environ Sci Technol* 40: 4353-4359.
33. Burke J (1970) *Cell Biology*. Williams and Wilkins Company, Baltimore :132-134.
34. Stearns RC, Paulauskis JD, Godleski JJ (2001) Endocytosis of ultrafine particles by A549 cells. *Am J Respir Cell Mol Biol* 24: 108-115.
35. Absolom DR, Zingg W, Neumann A (1987) Protein adsorption to polymer particles: Role of surface properties. *J Biomed Mater Res* 21: 161-171.
36. Cedervall T, Lynch I, Foy M, Berggard T, Donnelly S, et al. (2007) Detailed identification of plasma proteins adsorbed on copolymer nanoparticles. *Angewandte Chemie* 46: 5754-5756.